Electron-impact excitation of the $a\ ^3\Sigma_g^+$, $B\ ^1\Sigma_u^+$, $c\ ^3\Pi_u$, and $C\ ^1\Pi_u$ states of H_2

M. A. Khakoo* and S. Trajmar
Jet Propulsion Laboratory, California Institute of Technology, 4800 Oak Grove Drive, Pasadena, California 91109
(Received 7 February 1986)

Normalized differential and integral cross sections for electron-impact excitation of the dipole-allowed $B\ ^1\Sigma_u^+, C\ ^1\Pi_u$ and dipole-forbidden $a\ ^3\Sigma_g^+, c\ ^3\Pi_u$ states of molecular hydrogen have been determined by analysis of energy-loss spectra obtained with a crossed-beam apparatus at electron-impact energies of 20, 30, 40, and 60 eV and scattering angles ranging from 10° to 120°. Normalization of the data was achieved by utilizing the elastic differential cross sections measured previously by us (preceding article). The cross sections are compared with other available theoretical and experimental data.

I. INTRODUCTION

Electron-impact excitation of molecules is of fundamental importance in the understanding of the dynamics of planetary atmospheres, laser systems, and other weakly ionized plasmas.[1,2] This importance has stimulated considerable experimental and theoretical efforts. However, in comparison to electron-atom processes, inelastic electron-molecule scattering is in a relatively primitive stage. The only molecule for which reasonably extensive differential cross-section measurements have been made is N_2.[3] Theoretical models and calculations are not yet reliable.

To the case of molecular hydrogen, a special significance is attached because it is the simplest molecule and is therefore most amenable to a theoretical understanding of electron-scattering processes. Furthermore, there has been renewed interest in electron-impact excitation of H_2 due to the detection of intense auroral emission from Jupiter by Voyager I and II spacecraft.[4]

Most of the information concerning electron-impact excitation of the electronic states of H_2 is available in the form of excitation functions. A summary of the excitation functions of interest to us here is given by Trajmar *et al.*[5] These excitation functions when properly corrected for cascade contributions can be considered equivalent to integral electron-impact excitation cross sections. Significant extension of optical excitation functions to the vacuum ultraviolet (vuv) region was made in recent years. It seems now that the important cross section for production of Lyman α radiation by electron-impact excitation of H_2 has been well established.[6–9] This cross section has served as standard in most of the vuv optical excitation function measurements and the correction of its value will affect many of the vuv optical excitation data published previous to 1985.

The situation concerning actual electron-scattering measurements and differential cross sections (DCS's) for the excitation of electronic states of H_2 is very unsatisfactory. (See Ref. 5.) The study of differential (and to a certain extent, integral) electron-impact excitation of H_2 has been severely limited due to the difficulty in resolving the heavily overlapping band structure of the electronic transitions in the electron-energy-loss spectra. Previous work has been mainly on the $b\ ^3\Sigma_u^+$ continuum state of H_2 and the low-lying $B\ ^1\Sigma_u^+$ state of which the first three vibrational states are relatively free from any other overlapping state. Weingartshofer *et al.*[10] studied the $b\ ^3\Sigma_u^+$ and $B\ ^1\Sigma_u^+$ excitations at impact energies ranging from 10 to 16 eV and scattering angles from 10° to 120°. Hence, they observed the resonant excitation of the $B\ ^1\Sigma_u^+$ state through a series of resonances starting at 11.30 eV, whereas the $b\ ^3\Sigma_u^+$ state exhibited both resonant and nonresonant contributions. Trajmar *et al.*[11] studied the $b\ ^3\Sigma_u^+$ state at higher energies of 25 to 60 eV and normalized their data to Ochkur-Rudge theoretical calculations. Recently, Hall and Andric[12] measured the $b\ ^3\Sigma_u^+$ differential excitation functions from 0.2 to 2.2 eV above threshold for a 10-eV energy-loss value at scattering angles from 20° to 120° in order to investigate the shape resonance associated with the $^2\Sigma_g^+$ state as observed by Weingartshofer *et al.*,[10] but found no such effect, concluding that the DCS's were dominated by direct electron scattering. Recently, the DCS's for the $b\ ^3\Sigma_u^+$ state have been measured by Khakoo *et al.*[13] for electron-impact energies of 20 to 100 eV and scattering angles of 5°–130°.

Weingartshofer *et al.*[10] also studied the excitation of the $c\ ^3\Pi_u$, $e\ ^3\Sigma_u^+$, $g\ ^3\Sigma_g^+$, $d\ ^3\Pi_u$, $k\ ^3\Pi_u$, and $n\ ^3\Pi_u$ states of H_2 in the 10–16-eV impact energy region and determined absolute differential cross section (DCS) for the $c\ ^3\Pi_u$ ($v=1$) state at 10° in the 12.0–13.5-eV impact energy range.

Srivastava and Jensen[14] measured the differential cross section for the $B\ ^1\Sigma_u^+$ ($v=2$) energy-loss feature for impact energies of 15 to 60 eV, and scattering angles of 10° to 135°. Their normalization was based on the H_2 elastic DCS's which in turn was normalized by them to available He elastic DCS's. More accurate He DCS's became available since then and Trajmar *et al.*[7] have renormalized these DCS's.

At high (3 keV) energies, Geiger and Schmoranzer[15] studied H_2 energy-loss spectra with very high resolution ($\simeq$10 meV) and obtained relative optical excitation functions but no attempt was made to extract absolute cross sections from their data.

Differential and integral cross sections for excitation of

the electronic states of H_2 which are of interest to us here have been calculated recently by Rescigno *et al.*[16] (distorted wave, $a\,^3\Sigma_g^+$), Fliflet and McKoy[17] (distorted wave, $B\,^1\Sigma_u^+$), Arrighini *et al.*[18] (first Born, $B\,^1\Sigma_u^+$,$c\,^1\Pi_u$), Mu-Tao *et al.*[19] (distorted wave, $C\,^1\Pi_u$,$c\,^3\Pi_u$) and Lima *et al.*[20] (two-state close coupling, $a\,^3\Sigma_g^+$,$c\,^3\Pi_u$). Integral cross sections have been reported by Chung *et al.*[21] (Born-Rudge, $a\,^3\Sigma_g^+$,$c\,^3\Pi_u$), Chung and Lin[22] (two-state close coupling, $B\,^1\Sigma_u^+$, $a\,^3\Sigma_g^+$, and $c\,^3\Pi_u$), Arrighini *et al.*[23] (Born-Ochkur $B\,^1\Sigma_u^+$,$C\,^1\Pi_u$) and Hazi[24] (semiclassical impact parameter, $B\,^1\Sigma_u^+$).

We report here normalized DCS's for electron-impact excitation of the $B\,^1\Sigma_u$, $c\,^3\Pi_u$, $a\,^3\Sigma_g^+$, and $C\,^1\Pi_u$ states of H_2 in the range of impact energies (E_0) of 20–60 eV and scattering angles (θ) of 10°–120° at 10° intervals. These DCS data were determined by unfolding the energy-loss spectrum of H_2 in the energy-loss range of 11–14 eV using available Franck-Condon factors.[15,25] The method of acquiring the data, the unfolding data analysis, and the normalization procedures will be described. The data are compared to available differential and integral cross sections.

II. EXPERIMENTAL PROCEDURES

The electron spectrometer has been described previously.[26] The overall resolution of the spectrometer used in this work was about 40–50 meV for electron currents of 2–3 nA at the collision region. The incident beam divergence was estimated to be not greater than ±5° full width at half maximum (FWHM) at 20-eV impact energy, reducing to less than ±3° FWHM at 60-eV impact energy. An important feature of the detector (solid angle $\simeq\pm3°$ FWHM) was that its overall efficiency was to a good approximation independent of the electron-energy-loss value in the 11–14-eV energy-loss region for 20–60-eV impact energies. This was achieved by the application of a zoom lense in the electron density optics and by a tuning procedure. In this procedure the elastic and inelastic scattering signals were simultaneously optimized.

The gas target was provided by a hyperdermic needle of diameter 0.4 mm and length of 3.0 cm placed 3 mm from the electron-beam axis and at right angles to the scattering plane defined by the incoming and scattered electron beams. The target-gas source was operated with a drive pressure of approximately 3 Torr which gave a background pressure of 5×10^{-6} to 7×10^{-6} Torr in the experimental chamber. Backgrounds of 0.05 sec^{-1} corresponding to nearly dark channeltron counts were usually observed in this experiment. The contact potentials in the experiment were typically −0.5 eV as determined by repeatedly measuring the 19.3-eV resonance in He.

Data acquisition times for an energy-loss spectrum including the elastic and the 11–14-eV energy-loss region ranged from several hours to several days. Drift in the experimental conditions were averaged by multichannel scanning repeatedly over the elastic and inelastic features. A jump from the elastic to inelastic region was incorporated in the energy-loss scanning ramp voltage, which was controlled by the multichannel scalar (1024 channels at 0.1 sec per channel). The data was transferred from the multichannel scalar into a minicomputer for data analysis. Electron-energy-loss spectra with the elastic and inelastic features were taken at impact energies of 20, 30, 40, and 60 eV for the angular range of 10°–120°. At least three sets of spectra were taken at each impact energy and scattering angle. A typical spectrum is shown in Fig. 1.

III. DATA ANALYSIS

The data analysis followed closely the method used by Cartwright *et al.*[27] and the reader is referred to this article for extra details. The theory of the method is given by Bevington.[28] In this analysis, the excitation energies of the H_2 transitions and the vibrational Franck-Condon factors are assumed to be known. The rotational spacings in the spectra are significantly smaller than the best resolution encountered in this work ($\sim$15 meV as compared to 40 meV). The data, therefore, represent rotationally averaged DCS's. The contributions from the individual vibrational transitions to the overall electronic excitations are treated strictly on the basis of the Franck-Condon factors. The shape of the individual band features in the energy-loss spectra (mainly instrumental) has been assumed to be Gaussian and the width was determined by trial and error method. The width that gave the best fit to the experimental energy-loss spectrum was accepted. The signal at a given energy-loss value (ΔE) in the spectrum (for a fixed E_0 and θ values) consists of contributions from overlapping vibronic features and background scattering and it can be given as

$$S(E_0,\theta,\Delta E)=C\sum_{n'=0}^{N}\sum_{v'=0}^{M(n')}\sigma_{n',v'}(E_0,\theta)F_{n',v'}(\Delta E-\Delta E_{n',v'})$$
$$+B(E_0,\theta,\Delta E,\rho,I_0)\,, \tag{1}$$

where n' and v' are the electronic and vibrational quantum members characterizing the excited state corresponding to energy loss of $\Delta E_{n',v'}$, C is a constant related to the collision geometry, target density, electron-beam flux, and the detector efficiency, F is the line shape of the $n,v\rightarrow n',v'$ transition, N is the number of electronic states contributing to the spectrum and $M(n')$ is the number of vibrational levels for each electronic state, n'. The background contribution to the spectrum, B, is also dependent on the conditions in the collision region, i.e., the incident electron current I_0 and the target number density (ρ).

Within the Born-Oppenheimer approximation (nuclear-electronic mass separation) the relative vibrational intensities for a particular electronic level are independent of incident electron energy and hence we can write

$$\sigma_{n',v'}(E_0,\theta)=\sigma_{n'}(E_0,\theta)q_{v'}\,, \tag{2}$$

where $q_{v'}$ are the excitation Franck-Condon factors for the vibrational transitions. (The indexes associated with the initial state are suppressed since it is assumed that all transitions originate from the ground electronic and vibrational state.) $\sigma_{n'}$ now contains all information about the DCS's for a given electronic transition as a fraction of E_0 and θ. Thus the spectrum intensity in this approximation becomes

$$S(E_0,\theta,\Delta E)=C\sum_{n'=0}^{N}\sigma_{n'}(E_0,\theta)\sum_{v'=0}^{M(n')}q_{v'}F_{n',v'}(\Delta E-\Delta E_{n',v'})$$
$$+B(E,\theta,\Delta E,\rho,I_0)\ . \tag{3}$$

The background is described by a polynomial in energy loss

$$B(E_0,\theta,\Delta E,\rho,I_0)=\sum_{i=0}^{I}a_i(\Delta E)^i\ . \tag{4}$$

It was determined empirically for each spectrum based on the quality of the fit. In all cases it was well represented by a first- or second-order polynomial.

For the initial line-shape function a Gaussian width obtained from the elastic peak was chosen. It was found that this did not always provide the best fit to the spectra indicating different shape functions for elastic and inelastic transitions and/or that the spectrometer resolution did change with energy loss to some extent. However, the inelastic to elastic scattering intensity ratios were not very sensitive to this parameter. In any case for the evaluation of the spectra the width which gave the best fit was selected. Thus the line-shape function adopted can be written as

$$F_{n',v'}(\Delta E-\Delta E_{n',v'})=\frac{1}{\Delta\sqrt{\pi}}\exp\left[-\left[\frac{\Delta E-\Delta E_{n',v'}}{\Delta}\right]^2\right], \tag{5}$$

where Δ is the width of the Gaussian function.

The χ^2 value for the fit can be written as

$$\chi^2=\frac{1}{(D-k-1)}\sum_{j=1}^{D}\frac{(S_m^j-S^j)^2}{(\Delta S_m^j)^2}\ . \tag{6}$$

Here S_m^j and S^j are the measured and calculated signals, D is the number of data points, and k the number of parameters used in the fit, ΔS_m^j is the error associated with the S_m^j value (in this case the statistical error). Determination of a good fit for the spectrum in terms of $X_{n'}$ and a_i and Δ takes place by requiring that χ^2 be a minimum in a least squares sense, i.e.,

$$\sum_{n'}\frac{\partial\chi^2}{\partial X_{n'}}=0\quad(n'=1,\ldots,N)\ , \tag{7a}$$

$$\sum_{a_i}\frac{\partial\chi^2}{\partial a_i}=0\quad(i=1,\ldots,I)\ , \tag{7b}$$

$$\sum_{n'}\frac{\partial\chi^2}{\partial\Delta E_{n'}}=0\ , \tag{7c}$$

and

$$\frac{\partial\chi^2}{\partial\Delta}=0\ , \tag{7d}$$

where $X_{n'}=c\sigma_{n'}(E_0,\theta)$ are the relative differential cross sections for the overall electronic excitation. A good initial guess for the fitting parameters was important to avoid slow convergence. A good calibration of the energy loss scale for the spectrum using pronounced lines in the spectra was also important.

In order to obtain a set of good starting parameters for the iteration, we carried out a step-by-step fitting of individual electronic transitions. First the isolated (nonoverlapped) bands ($v'=0$ to 2) of the $B\,^1\Sigma_u^+$ excitation were fitted. The resulting value of the B-state relative cross sections were used together with the Franck-Condon factors to determine the relative cross sections for the higher-lying B ($v'>2$) excitations. A synthetic energy-loss spectrum for the B state was then generated and this was subtracted from the total experimental energy-loss spectrum. The procedure was then repeated for the next lowest-lying electronic state until all states had been accounted for. [See Fig. 2(a).] With the parameters obtained in the step-by-step procedure the original, experimental spectrum was then subjected to the fitting with $X_{n'}$ and a_i treated as free parameters and Δ held fixed. The program in this work used the gradient search method which reaches the conditions of Eq. (7) by changing the appropriate parameters simultaneously along the path of steepest change of χ^2 along a unit vector composed of the variables of Eq. (7). The method of gradient search has an advantage in than it approaches the minimum in χ^2 very rapidly, but it is slow in locating the precise position of this minimum, thus requiring a large number of iterations. However, it has the attractive advantage that it does not require the computation of large matrices compared to other methods. It took about ten iterations to converge to a statistically acceptable fit. Up to this point the resolution parameter (Δ) was left fixed. As the final steps of the fitting now this parameter was varied to improve the fit.

A typical experimental spectrum with the strong singlet transitions indicated is shown in Fig. 1. Some deviations between the observed and fitted spectra can be seen in the difference spectrum and are due to deviations of the instrumental profile from Gaussian shape, noise in the data, small error in the energy scale, and to the digital nature of the data. [See Fig. 2(b).] Effects related to the fact that each vibrational excitation took place at a slightly different impact energy above its own threshold and that the corresponding cross sections are associated with slightly different points on the cross section versus energy curve were neglected in the present fitting. At high and intermediate impact energies this neglect is justified for all practical purposes (if no resonances are present) but at low impact energies the spectrum can be seriously distorted by this effect and each vibrational excitation feature has to be treated individually.

The analysis requires the knowledge of the Franck-Condon factors and excitation energies for various vibronic states from the ground $X\,^1\Sigma_g^+$ state. The Franck-Condon factors together with the corresponding sources of these values are listed in Table I. Franck-Condon factors for the $c\,^3\Pi_u$ and $a\,^3\Sigma_g^+$ states were obtained from RKR (Rydberg-Klein-Rees) calculations of Cartwright[25] and for the $B\,^1\Sigma_u^+$ and $C\,^1\Pi_u$ states from Geiger and Schmoranzer.[15] In all cases the excitation energies were taken from the compilation of Sharp.[29]

The energy-loss spectra were fitted usually up to 14 eV using additional data for the $e\,^3\Sigma_u$ and $E\,^1\Sigma_g^+$ (Sharp[29]

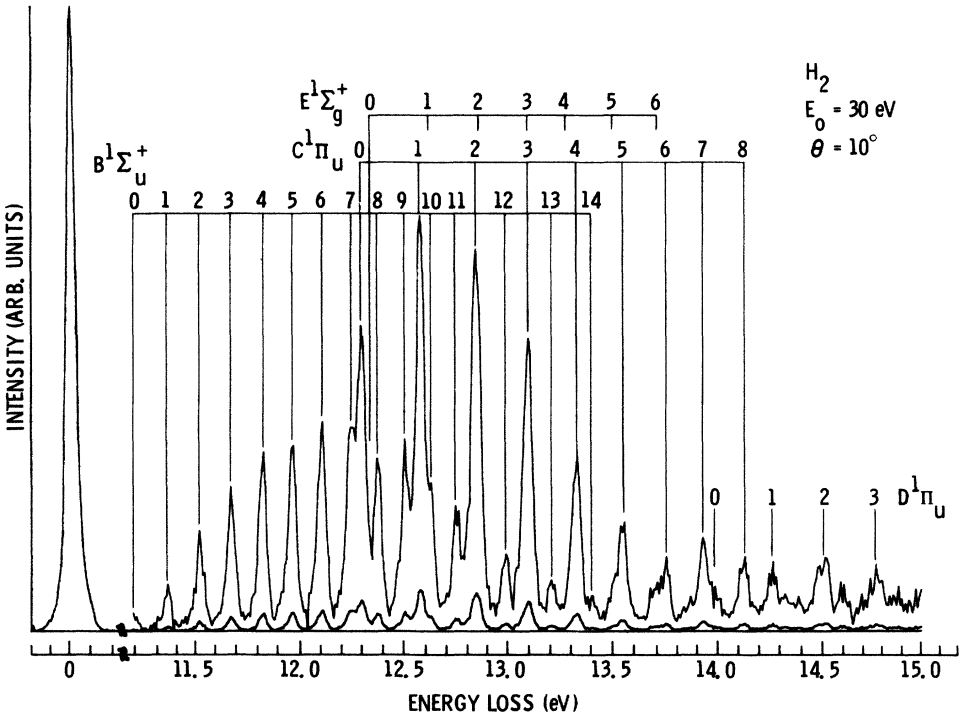

FIG. 1. Typical energy-loss spectrum of H_2. The prominent singlet state excitations are indicated.

TABLE I. Franck-Condon factors for excitation of the $X\,^1\Sigma_g^+$, $v=0$ state of H_2.

v'	$B\,^1\Sigma_u^+$ [a] Ref. 15	$c\,^3\Pi_u$ Ref.25	$a\,^3\Sigma_g^+$ Ref. 25	$C\,^1\Pi_u$ [a] Ref. 15	$E\,^1\Sigma_g^+$ Ref. 25	$e\,^3\Sigma_u^+$ Ref. 25
0	(0.0062)[b]	0.114	0.207	0.130	0.160	0.0438
1	0.020	0.186	0.255	0.216	0.208	0.0936
2	0.036	0.186	0.202	0.198	0.174	0.121
3	0.059	0.151	0.134	0.153		0.123
4	0.074	0.109	0.0814	0.116		0.111
5	0.083	0.074	0.0477	0.074		0.0920
6	0.091	0.048	0.0276	0.051		0.0729
7	0.091	0.032	0.0161	(0.033)		0.0537
8	0.078	0.020	0.0095	(0.021)		
9	0.074	0.011	0.0050	(0.014)		
10	0.067	0.005		(0.0089)		
11	0.059			(0.0057)		
12	0.050			(0.0036)		
13	0.041			(0.0018)		
14	0.033					
15	0.026					
16	0.022					
17	0.019					
18	0.017					
19	0.013					
20	0.010					
21	(0.009)					
22	(0.008)					
23	(0.007)					
24	(0.006)					

[a]The numbers in parentheses were obtained by extrapolation using the calculated values of Cartwright (Ref. 25).

[b]Obtained from electron-impact energy-loss spectra.

and Cartwright[25]) and the $B'\,^1\Sigma_u^+$ (Sharp[29] and Spindler[30]) states. Above 13 eV, however, the fitting became difficult and ambiguous because of the large number of states. We therefore restricted the present analysis to the 11–13.0-eV energy-loss region and to the *B*, *C*, *a*, and *c* states (see Fig. 2). Although the $E\,^1\Sigma_g^+$ state falls in this region and was included in the analysis, we do not report the cross sections for it. These cross sections are inaccurate due to the overlap of the *E*-state bands by the very strong *C*-state bands.

The normalization of the relative inelastic DCS's obtained from each energy-loss spectrum was achieved through the elastic scattering cross section. For this purpose we used the recent elastic scattering cross section of Khakoo and Trajmar (preceding article[26]). The factor that normalized the measured relative elastic scattering cross sections to the absolute scale was also used to normalize the inelastic data. The resulting differential cross sections are listed in Table II. Extrapolation to 0° and to 180° and integration overall angles yielded the integral cross sections of Table III. For the extrapolation we used as a guide theoretical DCS behavior whenever it was available. The estimated error limits for the differential and integral cross section are summarized in Table IV. The total error was calculated as the square root of the sum of the squares of the contributing errors.

IV. RESULTS AND DISCUSSION

A. $X \rightarrow B$ transition

The DCS's obtained in the present work are given in Table II(a) and shown and compared with other experimental and theoretical results in Figs. 3(a)–3(d). The data of Srivastava and Jensen[14] as renormalized by Trajmar *et al.*[5] are in excellent agreement with those of the present work, at all energies and most angles. At 20-eV impact energy, the two measurements show slight disagreement at larger scattering angles while in the case of 30, 40, and 60 eV the disagreements are found at the small scattering angles and in particular for the 10° DCS value. At 20-eV impact energy, as shown in Fig. 3(a), the first Born and Born-Ochkur model calculations of Arrighini *et al.*[18] predict a rather incorrect DCS behavior. The distorted-wave calculations of Fliflet and McKoy[17] show remarkably good agreement in shape with the present measurements but the absolute values obtained by them are somewhat larger.

The shoulder at the intermediate angles in these DCS values moves in smoothly with impact energy, starting out at 50° at 20-eV impact energy and getting to 40° at 60-eV impact energy indicating the increasing role of high partial waves in the scattering process as the impact energy increases. The distorted-wave calculations predict the right shape and reasonably correct magnitude for the DCS's at these energies. [See Figs. 3(b)–3(d).]

The available integral cross sections for the *B* state are compared in Fig. 4. The two-electron scattering data (present work and Srivastava and Jensen[14] as renormalized by Trajmar *et al.*[5]) agree within the experimental-error limits but the latter are consistently lower. The largest deviation is found at 60-eV impact energy. It is interesting

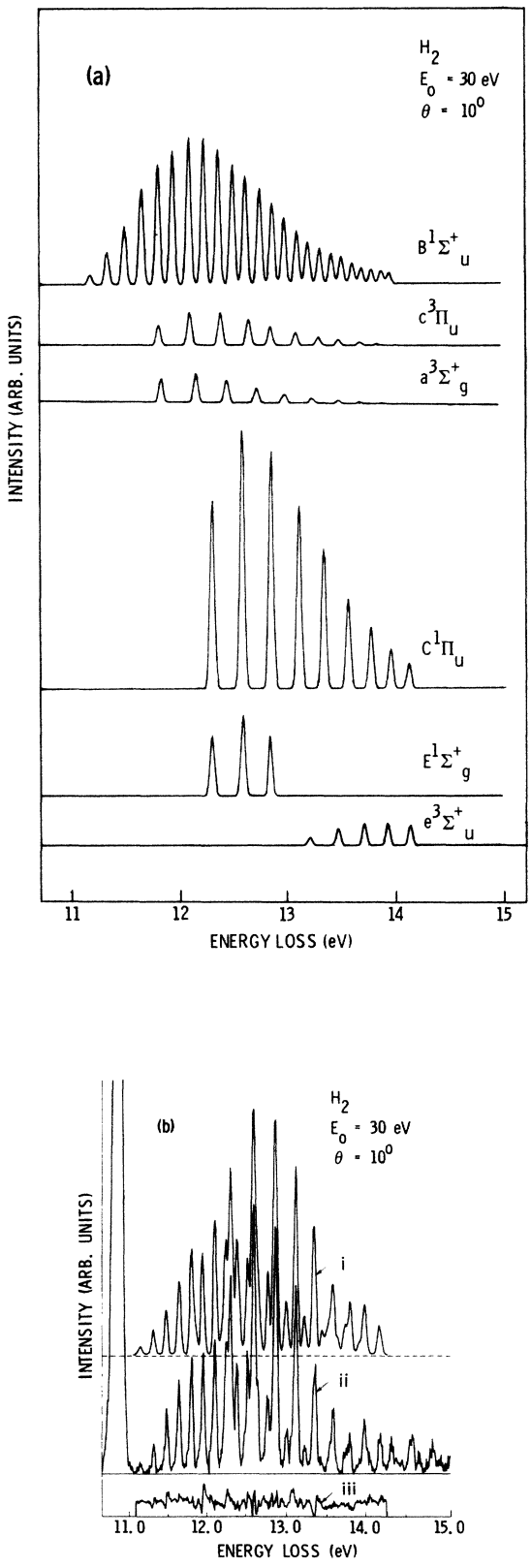

FIG. 2. (a) Computer decomposition of the spectrum of Fig. 1 into contributions from various electronic state excitations. (b) Comparison of the fitted (i) and the experimental (ii) spectra. The difference spectrum (iii) is also shown.

TABLE II. Differential cross sections for the (a) $B\,^1\Sigma_u^+$, (b) $c\,^3\Pi_u$, (c) $a\,^3\Sigma_g^+$, and (d) $C\,^1\Pi_u$ state excitation (10^{-18} cm^2/sr).

Scattering angle (deg)	Impact energy (eV) 20	30	40	60
	(a) $B\,^1\Sigma_u^+$			
10	18.6	41.8	66.8	86.3
20	8.99	10.7	19.8	7.22
30	4.26	3.61	5.02	1.86
40	2.77	2.23	1.83	0.888
50	2.05	1.59	0.918	0.564
60	1.55	1.15	0.644	0.424
70	1.20	0.920	0.545	0.218
80	0.927	0.755	0.433	0.204
90	0.783	0.623	0.350	0.133
100	0.621	0.504	0.252	0.110
110	0.508	0.372	0.197	0.100
120	0.490	0.316	0.151	0.093
	(b) $c\,^3\Pi_u$			
20	2.69	1.91	0.927	0.263
30	2.65	1.15	0.755	0.200
40	2.40	0.661	0.336	0.184
50	1.85	0.540	0.178	0.103
60	1.52	0.282	0.132	0.064
70	1.32	0.230	0.088	0.045
80	1.10	0.166	0.056	0.024
90	0.927	0.170	0.060	0.026
100	0.743	0.175	0.058	0.024
110	0.656	0.182	0.078	0.030
120	0.601	0.193	0.085	0.036
	(c) $a\,^3\Sigma_g^+$			
10		1.04	0.399	0.159
20	2.15	0.780	0.342	0.088
30	2.41	0.353	0.146	0.045
40	1.85	0.214	0.070	0.041
50	1.18	0.192	0.076	0.031
60	0.772	0.211	0.060	0.034
70	0.654	0.190	0.063	0.026
80	0.580	0.211	0.064	0.020
90	0.495	0.238	0.081	0.015
100	0.431	0.262	0.062	0.011
110	0.432	0.287	0.071	0.012
120	0.450	0.296	0.076	0.009
	(d) $C\,^1\Pi_u$			
10	13.4	25.2	48.1	114.0
20	7.23	5.77	8.16	4.72
30	3.64	1.69	1.05	0.622
40	1.45	1.04	0.613	0.298
50	0.930	0.722	0.466	0.203
60	0.743	0.580	0.369	0.180
70	0.676	0.543	0.312	0.145
80	0.660	0.469	0.282	0.135
90	0.581	0.407	0.260	0.131
100	0.539	0.370	0.255	0.130
110	0.579	0.348	0.231	0.140
120	0.611	0.328	0.237	0.122

TABLE III. Summary of integral excitation cross sections (10^{-18} cm^2)

Impact energy (eV)	State $B\,^1\Sigma_u^+$	$c\,^3\Pi_u$	$a\,^3\Sigma_g^+$	$C\,^1\Pi_u$
20	21.24	14.69	10.06	15.58
30	24.37	4.56	3.56	17.60
40	30.37	2.13	1.11	19.61
60	29.51	0.818	0.305	22.20

to note, however, that by raising the low-angle DCS's of Srivastava and Jensen to the present values which are about a factor of 3 higher, the integral cross sections come to an excellent agreement. This indicates that in the Srivastava and Jensen measurements some direct beam contribution may have been present which resulted in smaller inelastic to "elastic" scattering intensity ratios and, therefore, in smaller inelastic cross section. The present experimental results are in excellent agreement with cross sections derived from optical excitation measurements of Shemansky *et al.*[7] (which is based on the newly established Lyman-α cross sections and represents a correction to the previously published results of Ref. 31). The cross sections obtained from optical excitation functions by Malcolm *et al.*[32] (normalized to the old Lyman-α data[33]) and corrected for cascade polarization effects by McConkey[34] also fall into the same group as the previously discussed cross sections but they are somewhat smaller. Theoretical calculations of Chung *et al.*[21] (Born-Ochkur), Chung and Lin[22] (two-state close coupling), Fliflet and McKoy[17] (distorted wave) and Hazi[24] (semiclassical impact parameter) all yielded integral cross sections which are in reasonable agreement among each other but by about a factor of 2 higher than the experimental cross sections. It seems desirable, therefore, to carry out the close-coupling calculations with more channels involved. Such efforts are in progress now.[35]

TABLE IV. Estimated percent errors associated with the differential and integral cross sections (see text for explanation).

	Impact energy (eV) 20	30	40	60
Elastic DCS	12%	13%	13%	14%
Instrument transmission	10%	10%	10%	10%
Fitting error	8%	9%	10%	10%
Franck-Condon factors	4%	4%	4%	4%
Total error for inelastic DCS	18%	19%	20%	20%
Extrapolation	5%	5%	5%	5%
Total errors for integral cross sections	19%	20%	20%	21%

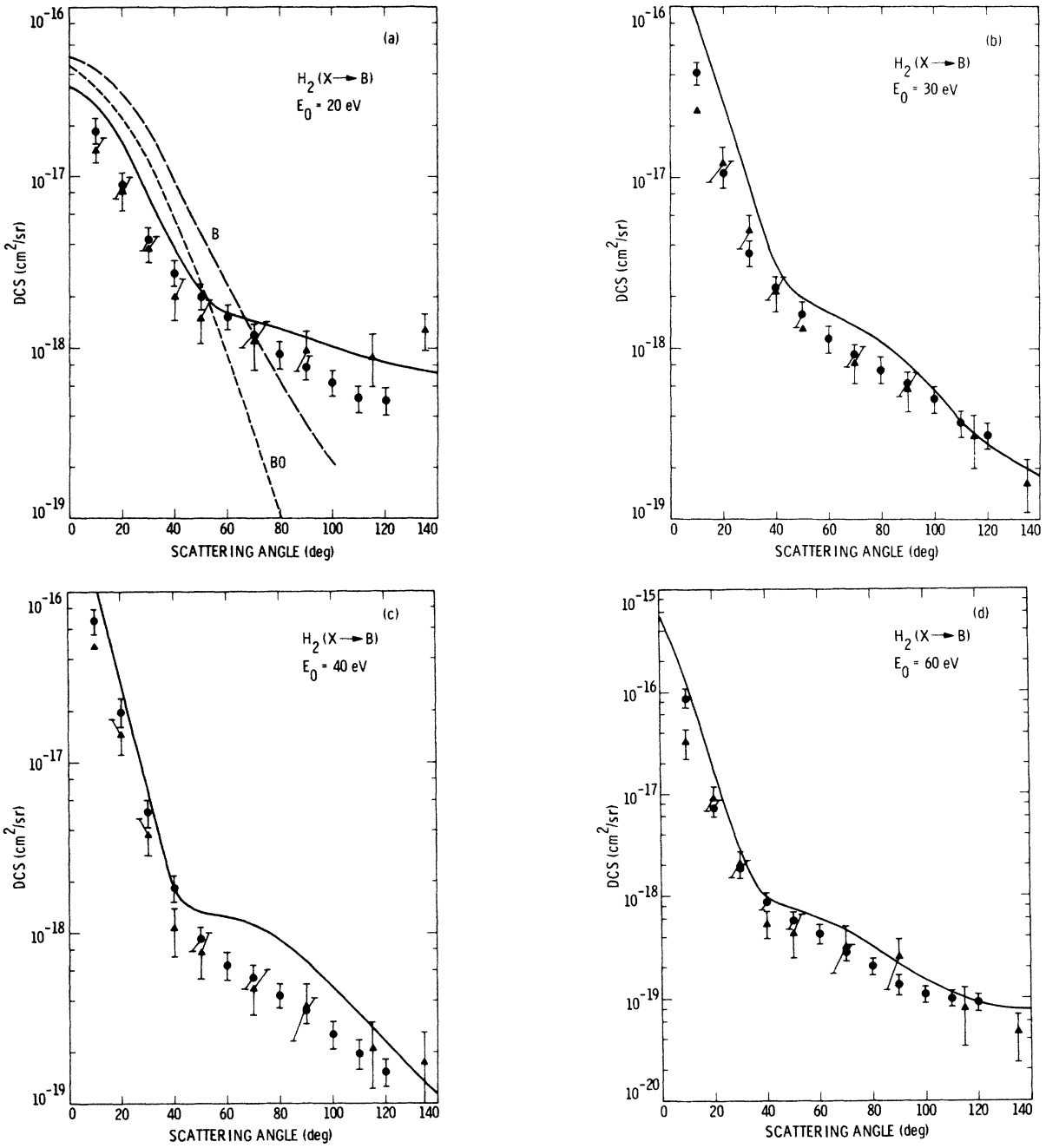

FIG. 3. (a) DCS for excitation of the $B\,^1\Sigma_u^+$ state at 20 eV impact energy. ϕ, present results; △, Srivastava and Jensen (Ref. 14) as renormalized by Trajmar *et al.* (Ref. 5); — — —, Arrighini *et al.* [Born (B), Ref. 18]; -----, Arrighini *et al.* [Born-Ochkur (BO), Ref. 18]; ——, Fliflet and McKoy (Ref. 17). (b) Same as Fig. 3(a) except $E_0=30$ eV. (c) Same as Fig. 3(a) except $E_0=40$ eV. (d) Same as Fig. 3(a) except $E_0=60$ eV.

B. $X \rightarrow c$ transition

The differential cross sections for this transition are summarized in Table II(b) and shown in Fig. 5 at 20-eV impact energy. No other experimental data are available to which the present results could be compared to. Theoretical calculations by Mu-Tao *et al.*[19] (distorted wave) and Lima *et al.*[20] (two-state close coupling) yielded very similar shapes for the DCS's as those found by us experimentally. In magnitude, however, the results of Lima *et al.* are about a factor of 3 higher while the results of Mu-Tao are about a factor of 3 lower than the present cross sections. Similar is the situation at 30 eV for the present and the Lima *et al.* results and at 60 eV for the present and Mu-Tao results (not shown).

Integral cross sections obtained from the present DCS's and those calculated by Chung *et al.*[21] (Born-Rudge approximation), Chung and Lin[22] (two-state close-coupling

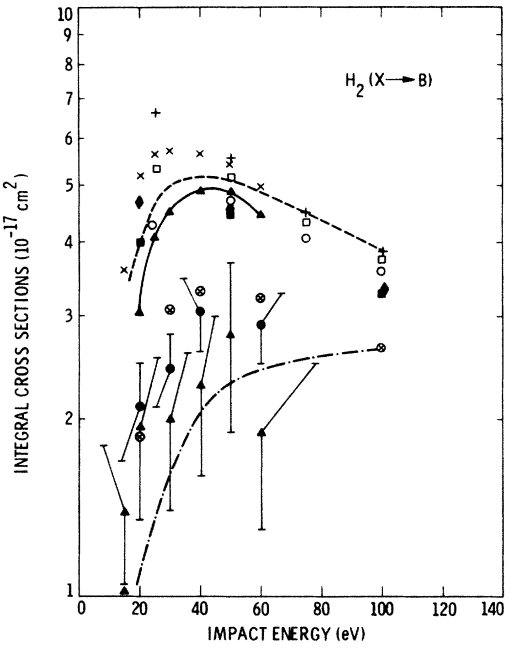

FIG. 4. Integral cross sections for the excitation of the $B\,^1\Sigma_u^+$ state. ⧫, present work (exp.); ⧫, Srivastava and Jensen (exp., Ref. 14) as renormalized by Trajmar *et al.* (Ref. 5); ⊗, Shemansky *et al.* (opt., Ref. 7; —·—·—·, Malcolm *et al.* (opt., Ref. 32) as corrected by McConkey (Ref. 34); +, Chung and Lin (Born, Ref. 22); □, Chung and Lin (Born-Ochkur, Ref. 22); ◆, Arrighini *et al.* (Born, Ref. 23); ■, Arrighini *et al.* (Born-Ochkur, Ref. 18); ○, Chung and Lin (two-state close coupling, Ref. 22); ×, Fliflet and McKoy (Born, Ref. 17); ▲, Fliflet and McKoy (distorted wave, Ref. 17); -----, Hazi (semiclassical impact parameter, Ref. 24).

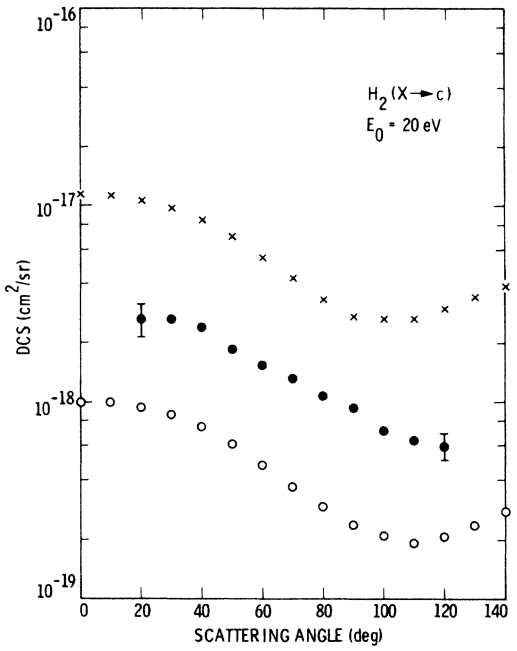

FIG. 5. DCS for excitation of the $c\,^3\Pi_u$ state at 20 eV impact energy. ●, present results; ×, Lima *et al.* (Ref. 20); ○, Mu-Tao *et al.* (Ref. 19).

approximation) and Mu-Tao *et al.*[19] (distorted wave) and Lima *et al.*[20] are shown in Fig. 6. The best agreement between the present results and theoretical calculations is found for the Born-Rudge model of Chung *et al.* This, however, must be fortuitous. The distorted-wave calculations of Mu-Tao *et al.* are also in reasonably good agreement with the present data at impact energies below 40 eV.

C. $X \rightarrow a$ transition

The differential cross sections are given in Table II(c) and a comparison of the present results with the calculations of Lima *et al.*[20] is shown in Fig. 7. The agreement between theory and experiment is excellent at 20 eV and good at 30 eV. No other DCS's are available to which the present results could be compared. The angular behavior is as expected: mildly forward peaking. In Fig. 8 the present integral cross sections are shown together with optical excitation function obtained by Ajello *et al.*[36] for the H_2 ($a \rightarrow b$) continuum radiation. Their relative curve was normalized to the present integral cross section at 20 eV. There is a very good agreement between their excitation function and the present cross section data at 30, 40, and 60 eV indicating that cascade contribution to the a state

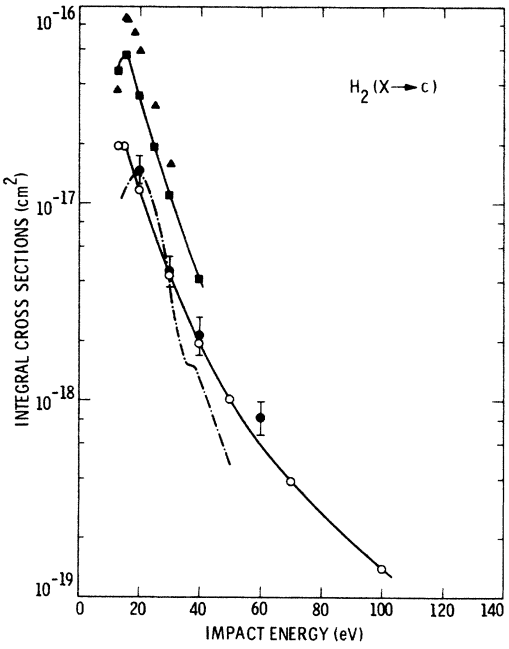

FIG. 6. Integral cross sections for the excitation of the $c\,^3\Pi_u$ state. ⧫, present results (exp.); —○—, Chung *et al.* (Born-Rudge, Ref. 21); —■—, Chung and Lin (two-state close coupling, Ref. 22); —·—·—·, Mu-Tao *et al.* (distorted wave, Ref. 19); ▲, Lima *et al.* (two-state close coupling, Ref. 20).

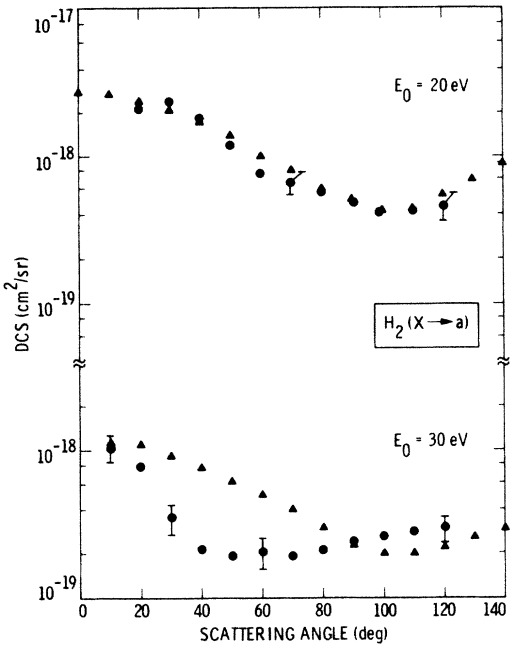

FIG. 7. Differential cross sections for the excitation of the $a\ ^3\Sigma_g^+$ state at 20 and 30 eV impact energies. ●, present results; ▲, Lima *et al.* (Ref. 20).

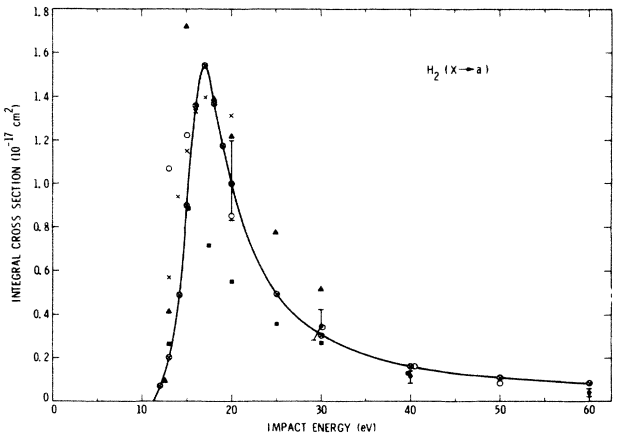

FIG. 8. Integral cross sections for the excitation of the $a\ ^3\Sigma_g^+$ state. ⊕, present results; ⊗, Ajello *et al.* (opt., Ref. 36); ○, Chung *et al.* (Born-Rudge, Ref. 21); ■, Chung and Lin (two-state close coupling, Ref. 22); ×, Rescigno *et al.* (distorted wave, Ref. 16); ▲, Lima *et al.* (two-state close coupling, Ref. 20).

are either negligible or in the same proportion at impact energies from 20 to 60 eV. The result of the calculations of Chung *et al.*[21] (Born-Rudge), Chung and Lin[22] (two-state close coupling), Rescigno *et al.*[16] (distorted wave) and Lima *et al.*[20] (two-state close coupling) are also shown. At impact energies below 30 eV there is a substantial disagreement among various theoretical results and between theory and experiment. At higher energies the Born-Rudge model cross sections agree well with the present results.

D. $X \rightarrow C$ transition

The DCS's for this transition are strongly forward peaked and values of the DCS's increase with increasing impact energy at small scattering angles while the reverse is true at large scattering angles. The cross over occurs at about 20° where the DCS value is nearly independent of impact energy (for the energies that we are concerned with). The differential cross sections are given in Table II(d) and compared with the Born and Born-Ochkur calculations of Arrighini *et al.*[18] at 20 eV and with the distorted-wave calculations of Mu-Tao *et al.*[19] at 20- and 60-eV impact energies in Fig. 9. The DCS curves of experiment and theory show some resemblance to each other but substantial disagreement are present in absolute values.

The integral cross sections are compared with other available data in Fig. 10. The values obtained from optical excitation measurements by Shemansky *et al.*[7] are in good agreement with the present data except at 20-eV impact energy. The theoretical results are about a factor of 2 higher than the experimental data.

V. REMARKS AND SUGGESTIONS FOR FURTHER WORK

The present cross sections were derived from energy-loss spectra and normalized with respect to elastic scattering. An initial step-by-step fitting of successive individual transitions and then a fitting of the combined transitions

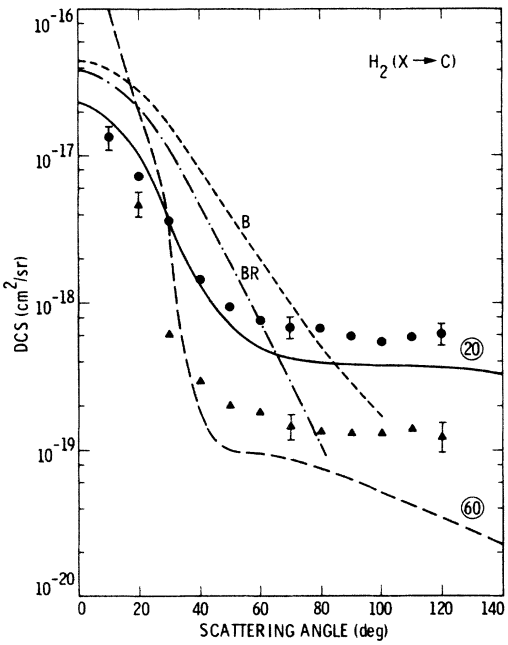

FIG. 9. Differential cross sections for the excitation of the $C\ ^1\Pi_u$ state at 20 eV impact energy; ●, present results; -----, Arrighini *et al.* [first Born (B), Ref. 18)]; —·—·—·, Arrighini *et al.* [Born-Rudge (BR), Ref. 18]; ——, Mu-Tao *et al.* (distorted wave, Ref. 19) and at 60 eV impact energy; △, present results; — — —, Mu-Tao *et al.* (distorted wave, Ref. 19).

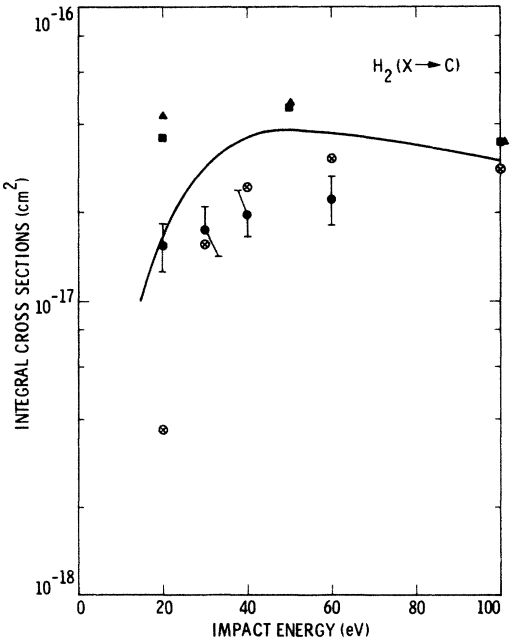

FIG. 10. Integral cross sections for the excitation of the $C\,^1\Pi_u$ state: ●, present results; ⊗, Shemansky *et al.* (Ref. 7); △, Arrighini *et al.* (Born, Ref. 23); ■, Arrighini *et al.* (Born-Ochkur, Ref. 18); ——, Mu-Tao *et al.* (distorted wave, Ref. 19).

was applied. This procedure was found to be quite feasible even when a large number of overlapping vibrational structures are present. In the unfolding procedure it was assumed that the scattering intensities associated with the vibrational bands of electronic transitions in the energy-loss spectra were strictly proportional to the Franck-Condon factors. This is a good approximation of high and intermediate impact energies where distortions from the Franck-Condon distribution due to threshold and resonance effects can be neglected. At low impact energies, where the cross section changes fast with energy a distortion in the relative band intensities occurs since the individual bands in the energy-loss spectra are excited at different energies above their own thresholds. This effect was demonstrated recently for N_2 Lyman-Birge-Hopfield Band system by Ajello and Shemansky.[37] Our 20-eV results may have been influenced by this near-threshold effect, but not significantly. It is desirable to extend these electron-scattering cross-section measurements to lower impact energies. The calibration techniques, as mentioned before, and the unfolding procedure required at the low energies are more involved but feasible with present capabilities. Such measurements are under way in our laboratory for N_2 and are planned for H_2.

In general, data derived from optical excitation functions (with the recently established Lyman-α cross section) agree well with the present results. This observation gives support to the correction in the Lyman-α cross section of references 6, 7, 8, and 9, of the previous measurement.[33]

First-order perturbation-type calculations give, in general, poor agreement with the experimental data (except in a few cases which should be considered fortuitous). Distorted-wave and two-channel close-coupling calculations show in general good qualitative agreement with measurements but there is a great deal more to be desired concerning quantitative agreement. It would be very important to extend the close-coupling calculations to include more channels and see what the effect of these inclusions would be. We would like to emphasize the importance of publishing differential cross sections obtained from theoretical calculations. This information is necessary to judge the reliability of the calculations against experiments and is very important for proper extrapolation of measured cross sections to the experimentally unavailable angular regions (near 0° and 180° regions) for the purpose of obtaining integral cross sections).

ACKNOWLEDGMENTS

The research described in this paper was carried out at the Jet Propulsion Laboratory, California Institute of Technology, and was sponsored by the National Aeronautics and Space Administration (NASA), the National Science Foundation, and NATO Scientific Affairs Division. One of the us (M.A.K.) received additional support from NASA and the National Research Council during the course of this work. We would like to express our gratitude to J. M. Ajello, D. C. Cartwright, J. Forand, T. L. Gibson, D. T. Hall, W. Huo, J. W. McConkey, V. McKoy, M. A. P. Lima, D. E. Shemansky, and J. M. Woolsey for valuable discussions and/or making available to us unpublished results. G. R. Steffensen contributed valuable help in setting up and carrying out these measurements.

*Present address: Physics Department, University of Windsor, 401 Sunset Avenue, Windsor, Ontario, Canada N9B 3P4.

[1]K. Takayanagi and Y. Itikawa, Space Sci. Rev. **11**, 389 (1970).

[2]S. Trajmar and D. C. Cartwright, in *Electron-Molecule Interactions and Their Applications,* edited by L. G. Christophorou (Academic, New York, 1984), Chap. 2.

[3]D. C. Cartwright, A. Chutjian, S. Trajmar, and W. Williams, Phys. Rev. A **16**, 1013 (1977); D. C. Cartwright, W. Williams, S. Trajmar, and A. Chutjian, *ibid.* **16**, 1041 (1977); A. Chutjian, D. C. Cartwright, and S. Trajmar, *ibid.* **16**, 1052 (1977).

[4]A. L. Broadfoot *et al.*, Science **24**, 979 (1979); **212**, 206 (1981); J. Geophys. Res. **86**, 8259 (1981).

[5]S. Trajmar, D. F. Register, and A. Chutjian, Phys. Rep. **97**, 219 (1983).

[6]B. van Zyl, M. W. Gealy, and H. Newmann, Phys. Rev. A **31**,

2922 (1985).
[7]D. E. Shemansky, J. M. Ajello, and D. T. Hall, Astrophys. J. **296**, 765 (1985).
[8]R. C. G. Ligtenberg, A. McPherson, N. Rouze, W. B. Westerweld, and J. S. Risley, Proceedings of the Sixteenth Annual Meeting of Division of Electron and Atomic Physics, American Physical Society, 1985, Norman, Oklahoma (unpublished).
[9]J. M. Woolsey, J. Forand, and J. W. McConkey (private communication).
[10]A. Weingartshofer, H. Erhardt, V. Herman, and F. Linder, Phys. Rev. A **2**, 294 (1970).
[11]S. Trajmar, D. G. Truhlar, J. K. Rice, R. T. Brinkmann, and A. Kuppermann, J. Chem. Phys. **49**, 5464 (1968).
[12]R. I. Hall and L. Andric, J. Phys. B **17**, 3815 (1984).
[13]M. A. Khakoo, S. Trajmar, R. McAdams, and T. Antoni (unpublished).
[14]S. K. Srivastava and S. Jensen, J. Phys. B **10**, 3341 (1977).
[15]J. Geiger and H. Schmoranzer, J. Mol. Spectrosc. **32**, 39 (1969).
[16]T. N. Rescigno, C. W. McCurdy, Jr., V. McKoy, and C. F. Bender, Phys. Rev. A **13**, 216 (1976).
[17]A. W. Fliflet and V. McKoy, Phys. Rev. A **21**, 1863 (1980).
[18]G. P. Arrighini, F. Biondi, and C. Guidotti, Mol. Phys. **41**, 1501 (1980).
[19]L. Mu-Tao, R. R. Lucchese, and V. McKoy, Phys. Rev. A **26**, 3240 (1982).
[20]M. A. P. Lima, T. L. Gibson, W. Huo, and V. McKoy (private communication).
[21]S. Chung, C. C. Lin, and E. T. P. Lee, Phys. Rev. A **12**, 1340 (1975).
[22]S. Chung and C. C. Lin, Phys. Rev. A **17**, 1874 (1978).
[23]G. P. Arrighini, F. Biondi, C. Guidotti, A. Biagi, and F. Marinelli, Chem. Phys. **52**, 133 (1980).
[24]A. N. Hazi, Phys. Rev. A **23**, 2232 (1981).
[25]D. C. Cartwright (private communication).
[26]M. A. Khakoo and S. Trajmar, preceding paper, Phys. Rev. A **34**, 138 (1986).
[27]D. C. Cartwright, A. Chutjian, S. Trajmar, and A. Williams, Phys. Rev. A **16**, 1013 (1977).
[28]P. R. Bevington, *Data Reduction and Error Analysis for the Physical Sciences* (McGraw-Hill, New York, 1969), pp. 215–219.
[29]T. E. Sharp, At. Data **2**, 119 (1971).
[30]R. J. Spindler, J. Quant. Spectrosc. Radiat. Transfer **9**, 1041 (1969).
[31]J. M. Ajello, D. Shemansky, T. L. Kwok, and Y. L. Yung, Phys. Rev. A **29**, 636 (1984).
[32]M. J. Mumma and E. C. Zipf, J. Chem. Phys. **55**, 1661 (1971).
[33]I. C. Malcolm, H. W. Dassen, and J. W. McConkey, J. Phys. B **12**, 1003 (1979).
[34]J. W. McConkey, J. Chem. Phys. **74**, 6224 (1981).
[35]T. L. Gibson, M. A. P. Lima, W. Huo, and V. McKoy (private communication).
[36]J. M. Ajello, K. D. Pang, B. Franklin, and F. Flam, Abstracts of the American Geophysical Union Fall Meeting, San Francisco, 1985 [EOS Transactions, Am. Geophys. Union **66**, 989 (1985)], private communication.
[37]J. M. Ajello and D. E. Shemansky, J. Geophys. Res. **90**, 9845 (1985).